biologics

MDPI

Article

Hydrolysates of Chicken Byproducts and Their Effect on the Histological and Histopathological Analysis of Liver and Kidney in a Murine Model of Induced Metabolic Syndrome

Martha Guillermina Romero-Garay [1], Efigenia Montalvo-González [1], Odila Saucedo-Cárdenas [2], Eduardo Mendeleev Becerra-Verdín [3], Adolfo Soto-Domínguez [2,*], Cristian Rodríguez-Aguayo [4,*] and María de Lourdes García-Magaña [1,*]

1 Integral Laboratory of Food Research, Tecnológico Nacional de México/Instituto Tecnológico de Tepic, Av. Tecnológico 2595 Col. Lagos del Country C.P., Tepic 63175, NA, Mexico; maguromeroga@ittepic.edu.mx (M.G.R.-G.); emontalvo@ittepic.edu.mx (E.M.-G.)
2 Histology Department, Facultad de Medicina, Universidad Autónoma de Nuevo León, Madero y E. Aguirre Pequeño SN, C.P., Monterrey 64460, NL, Mexico; odila.saucedocr@uanl.edu.mx
3 Clinical Research Laboratory and Histology, Universidad Autónoma de Nayarit, Ciudad de la Cultura "Amado Nervo" C.P., Tepic 63155, NA, Mexico; eduardo.becerra@uan.edu.mx
4 Department of Experimental Therapeutics, The University of Texas MD Anderson Cancer Center, Houston, TX 77030, USA
* Correspondence: ibqasoto@yahoo.com.mx (A.S.-D.); CRodriguez2@mdanderson.org (C.R.-A.); mgarciam@ittepic.edu.mx (M.d.L.G.-M.)

Abstract: This study investigated the potential of chicken byproduct hydrolysates (CBH) characterized by a mixture of low-molecular-weight peptides (<1.35 kDa) and larger peptides (<17.5 kDa) as a treatment for metabolic syndrome (MS), from a histological and histopathological point of view. This study aimed to evaluate the effects of CBH obtained using plant proteases (BP: *B. pinguin*, BK: *B. karatas*, BRO: bromelain) on the histological and histopathological analysis of the liver and kidney in an MS-induced murine model. Methods: Thirty adult male Wistar rats were randomly assigned to six groups (n = 5): (1) standard diet (STD); (2) MS with a hypercaloric diet (MS + HC); (3) CBH-BP (200 mg/kg of body weight); (4) CBH-BK (200 mg/kg of body weight); (5) CBH-BRO (200 mg/kg of body weight); (6) carnosine (CAR) 50 mg/kg of body weight. Liver and kidney samples were processed by conventional hematoxylin and eosin (H&E) histological techniques, Masson's trichrome stain (MTS), and the periodic acid–Schiff (PAS) histochemical method. A scoring scale was used for the histopathological evaluation with scores ranging from 0 (normal tissue) to 4 (severe damage). Results: CBHs demonstrated a significant therapeutic effect ($p < 0.05$) on hepatic and renal morphological alterations induced by MS. Hepatic scores for lipid inclusions, vascular congestion, and cellular alteration were all reduced to below two. Similarly, renal scores for tubular degeneration, vascular congestion, and dilation of Bowman's space were also decreased to less than two. The therapeutic efficacy of CBHs was comparable to that of the positive control, CAR (β-alanyl-L-histidine). Conclusions: CBH-BP, CBH-BK, and CBH-BRO treatments reduced morphological alterations observed in liver and kidney tissues, which is relevant since from a histological and histopathological point of view, it allows us to understand at the cellular and tissue level the effects that these treatments can have on a living organism, indicating a potential to improve organ health in people with MS.

Keywords: chicken byproduct hydrolysates; metabolic syndrome; plant proteases; liver and kidney; morphological alterations

Citation: Romero-Garay, M.G.; Montalvo-González, E.; Saucedo-Cárdenas, O.; Becerra-Verdín, E.M.; Soto-Domínguez, A.; Rodríguez-Aguayo, C.; García-Magaña, M.d.L. Hydrolysates of Chicken Byproducts and Their Effect on the Histological and Histopathological Analysis of Liver and Kidney in a Murine Model of Induced Metabolic Syndrome. *Biologics* **2024**, *4*, 345–363. https://doi.org/10.3390/biologics4030021

Academic Editor: Manfredi Tesauro

Received: 17 July 2024
Revised: 29 August 2024
Accepted: 11 September 2024
Published: 20 September 2024

1. Introduction

MS is a cluster of metabolic disorders characterized by abdominal obesity, dyslipidemia, hypertension, and hyperglycemia, representing a major global health challenge. Beyond its association with cardiovascular disease and type 2 diabetes mellitus, MS has

been linked to a broader spectrum of chronic diseases, such as non-alcoholic fatty liver disease, chronic kidney disease, cancer, and even reproductive health problems [1–4]. The prevalence of MS is increasing worldwide, affecting both developed and developing countries. Recent epidemiological studies estimate that between 20% and 25% of adults worldwide suffer from this condition [5,6]. The main factors causing this epidemic include the excessive consumption of energy-dense foods and a sedentary lifestyle [3]. It is noteworthy that a recent study conducted in a Latin American population revealed a high prevalence of MS among people over 40 years of age [6]. In addition, an increased prevalence of MS has been determined among men aged 30 to 40 years and women over 70 years [7]. Because chronic diseases account for 68% of global mortality, early detection and intervention in MS cases are crucial to mitigate their adverse health consequences [8]. In this sense, the incorporation of short-chain, low-molecular-weight peptides derived from different protein hydrolysates has been considered a therapeutic alternative for metabolic disorders such as diabetes mellitus and MS. However, the potential secondary effects generated by these molecules must be evaluated since they are presented as the new generation of biologically active regulators that can prevent oxidation and cellular inflammation [9,10].

On the other hand, chicken byproducts have been used in recent years to obtain bioactive peptides, due to the high protein concentration they present (80–90%), especially in tissues such as blood and viscera, positioning them as an attractive raw material for biotechnology [11]. Proteins such as hemoglobin, collagen, and keratin present in these by-products are candidates for the generation of bioactive peptides with various applications [11,12]. In this regard, the physiological activities of peptides derived from hydrolysates of poultry byproducts showed antioxidant and antihypertensive effects, lipid regulation, and protective effects in the liver, which have shown mainly through in vitro analysis, cultured cells, and animal studies [13]. Likewise, pepsin-digested chicken liver hydrolysates (CLH) have shown hepatic-modulatory effects on autophagy regulation against liver fibrogenesis in male Wistar rats [14], decreased hepatosteatosis in high-fat diet (HFD) mice [15], demonstrated protective effects against kidney damage, cardiac fibrosis, and inflammation in mice fed with a high-fat diet (HFD) [16], alcoholic fatty liver in mice [17] and liver fibrogenesis in rats [18], and showed antioxidant effects in vitro [13,19,20].

Additionally, enzymes from BP and BK could be a source of peptides with potential applications. It has been shown that their use allows obtaining the low molecular weight (<1.35 kDa) of antioxidant peptides [13] and can generate health effects on biochemical markers in MS-induced male Wistar rats [21]. However, more research is needed to explore their potential to produce peptides with antioxidant properties and possible health benefits. From a therapeutic point of view, histological and histopathological analysis plays a crucial role in the investigation of the possible effects of CBHs, since it allows us to visualize and evaluate changes at the cellular and tissue level that occur in response to their intake. This information is essential to understand the mechanisms of action of CBHs. Therefore, this study aimed to evaluate the possible effect of CBHs obtained with semi-purified proteases from *B. pinguin* and *B. karatas* on the histological and histopathological analysis of the liver and kidney in an MS-induced murine model. Analysis of liver and kidney tissues was performed employing histological techniques, to evaluate if HPO, particularly when obtained with BP, BK, or BRO proteases, may offer a therapeutic approach for MS, indicating a potential agent to improve the health of altered organs in people with MS.

2. Materials and Methods

2.1. Obtention of Chicken Byproduct Hydrolysates (HPO)

Extraction and pre-purification of the enzymes from the fruits of BP and BK were performed according to the methodologies described by García-Magaña et al. [22] and Romero-Garay et al. [13]. The pre-purified enzymes from BP and BK presented a specific enzymatic activity of 6.24 AU/mg and 4.76 AU/mg, respectively. These enzymes were applied to chicken byproducts to obtain hydrolysates according to the methodology proposed by Romero-Garay et al. [13]. Chicken byproducts were homogenized in 0.2 M of

sodium phosphate buffer, pH 6.5, at a ratio of 1:20 (*w*/*v*). The homogenate was subjected to heat treatment at 100 °C for 15 min and then cooled. Subsequently, individual enzymatic hydrolyses were performed using the enzymatic extracts of BP, BK, and BRO. For each hydrolysis, 1 mL of enzyme solution (100 µg/mL) was added to the homogenate and incubated under the following conditions: 40 °C for 30 min at pH 6.5 (CBH-BP), 25 °C for 4 h at pH 6.5 (CBH-BK), and 37 °C for 4 h at pH 7.0 (CBH-BRO). After the incubation time, the enzymatic reaction was stopped by heating at 100 °C for 15 min. The hydrolysates obtained were centrifuged at 14,000× *g* at 4 °C for 10 min (Hermle, Z32HK, Wehingen, Germany) and filtered through 0.45 µm membranes (Millipore, MF-Membrane Filtres HAWP, Merck Millipore, Darmstadt, Alemania). The obtained hydrolysates were frozen at −20 °C and lyophilized for later use.

2.2. Animals and Diet Administered for the Induction of Metabolic Syndrome (MS)

In the present study, 30 male Wistar rats (8–10 weeks old) weighing 110 ± 30 g were obtained from BIOINVERT (Mexico D.F). They were kept in a 12 h light/12 h dark cycle, at a temperature of 23 ± 1 °C and 60 ± 10% relative humidity. The rats were housed in individually ventilated cages with a 12 h light/12 h dark cycle, maintained at a temperature of 23 ± 1 °C and 60 ± 10% relative humidity. The experimental protocol (M00.2./471/2019) was approved on 11 March 2019, by the National Technological Institute of Mexico/Technological Institute of Tepic, Nayarit, Mexico; likewise, the State Bioethics Committee of Nayarit, Mexico approved the experimental protocol (No. CENB/03/2017) used in the present investigation, and the protocols of the Institutional Committee for the Care and Use of Animals were performed according to Mexican standards (NOM-062-ZOO-1999, 2017). During the first week, the animals had free access to a standard diet (STD) with 49% carbohydrates (*w*/*w*), 23% protein (*w*/*w*), 3% fat (*w*/*w*), 6% fiber (p/p), and 7% ash (p/p) (Nutricubo Purina®), and water to allow their adaptation to the environment.

For the generation of the MS model and the experimental design, the methodology proposed by Romero-Garay et al. [21] was followed. After a week of acclimatization, the animals were randomly assigned to six groups of rats (n = 5). The control group (1) continued the STD. For groups 2–6 with MS, a high-calorie diet (HC) was formulated from the standard diet (STD), to which the following components were added: 19% lard to increase lipid content, 12% refined sugar to increase caloric intake, and 11% egg as a binder. This formulation resulted in a high-calorie diet that served as a model for MS. In addition, rats received two intraperitoneal injections of 40 mg/kg of rat weight administered into the abdominal cavity of Streptozotocin (STZ, Sigma-Aldrich, St. Louis, MO, USA) dissolved in 1.5 mL of citrate buffer (pH 4.5). The doses were applied once a week. After the induction period, a glucose tolerance curve was performed to confirm the development of diabetes.

2.3. Experimental Design

The experimental design was as follows after the initial 5 weeks of induction: Group 1 continued with the SDT diet; Group 2: MS + HC; Group 3: MS + CBH obtained from BP (CBH-BP: 200 mg/kg); Group 4: MS + CBH obtained from BK (CBH-BK: 200 mg/kg); Group 5: MS + CBH obtained from BRO (CBH-BRO: 200 mg/kg); Group 6: MS + Carnosine (MS + CAR: 50 mg/kg). Oral doses of CBH were dissolved in water for human consumption and administered in 0.3 mL doses.

At the end of the experiment (10 total weeks), the euthanasia protocol was followed following the Manual on the Use and Care of Experimental Animals (NOM-062-ZOO-1999, 2017). The liver and kidney tissue samples were collected immediately and fixed in a Formol 10% solution (*v*/*v*) for further histological analysis.

2.4. Histological Analysis

2.4.1. Sample Processing

The liver and kidney samples were processed using the conventional histological technique and dehydrated with gradual ethanol solutions (60°, 70°, 80°, 96°, absolute, or 100%) until the inclusion of the samples in paraffin blocks with a KEDEE automatic tissue processor (KD-TS3A, Hangzhou, China).

2.4.2. Final Fixation

The final fixation was carried out using Tissue Embedding Center (KD-BM, KEDEE®) equipment. The pre-included tissue was fixed in liquid paraffin to form the tissue blocks that provided support for subsequent cutting. Immediately after forming the blocks, they were placed on a cooling plate (KD-BL, KEDEE®).

2.4.3. Sectioning

Five μm sections were obtained using a Leica microtome (RM2125RTS, Nussloch, Germany). Before sectioning, the blocks were placed on a cooling plate to facilitate sectioning and to prevent the paraffin from contracting and generating an artifact.

2.4.4. Floating and Adhesion

Once the sections were obtained, they were spread in a hot bath (KD-P, KEDEE®) at 40–45 °C with gelatin, which helped each section adhere to the slide. This procedure was performed on all blocks, obtaining 1 slide per section/organ/rat.

2.4.5. Dewaxing and Hydration

Before staining, the slides were placed in a drying oven for 30 min, then removed and allowed to cool. For dewaxing, the slides were immersed in xylene for 5 min. Predrying accelerates the dissolution of the paraffin and reduces the immersion time in xylene. Subsequently, to carry out hydration, the slides were immersed in pure xylene for 5 min, xylene–ethanol 1:1 (v/v) for 5 min, absolute ethanol for 2 min, 96% ethanol for 2 min, and rinsed with distilled water for 1 min. In this way, water was restored to the tissues, and the slides were ready to be stained.

2.4.6. Histochemical Stains

Hematoxylin and Eosin (H&E)

The 5-μm thick histological slides were stained with H&E to evaluate the general histology of the liver and kidney. Histological sections were hydrated and subjected to a conventional staining protocol. Gill's hematoxylin (2 min) was used to stain the nuclei and eosin (1 min) to visualize the cytoplasm. Subsequently, washes were carried out with running water, acid alcohol, ammonia water, and ethyl alcohol in increasing concentrations. Finally, they were cleared with xylene and mounted in resin.

Masson's Trichrome Stain (MTS)

The MTS allowed us to evaluate the connective tissue of these organs related to fibrosis. Histological sections of 5 μm, previously hydrated, were fixed in Bouin's solution (30–60 min at 56 °C). Subsequently, the nuclei were stained with Weigert's ferric hematoxylin (10 min), the cytoplasm with Biebrich scarlet fuchsin (1 min), and the collagen fibers with aniline blue (1 min). After differentiation with acetic acid and dehydration in a series of alcohols and xylene, they were subsequently mounted in resin.

Periodic Acid–Schiff (PAS)

We employed the histochemical method to analyze the glycogen inclusions in the liver as well as the identification of complex polysaccharides of the basal membrane in the kidney [15]. Histological sections of 5 μm were oxidized with 0.5% of periodic acid (5–10 min) and then treated with Schiff's reagent (20 min) to demonstrate the presence of

polysaccharides. The nuclei were then counterstained with Gill's hematoxylin (1–2 min). After dehydration in a series of alcohol and clearing in xylene, they were mounted in resin.

Sections were analyzed, and high-resolution images were obtained using an OMAX digital optical microscope (M837ZL-C180U3, Kent, WA, USA) coupled to an OMAX photographic camera (A3518003) using OMAX Toop View software version 3.7.

2.5. Morphometrical Analysis of the Histopathological

For the evaluation of damage, the following scoring scale was used according to Altınkaynak et al. [16]. This scoring scale was used for the histopathological evaluation of both the liver and kidney: 0 = normal tissue (no damage), 1 = minimal damage (<25% damage), 2 = light damage (25–50% damage), 3 = medium damage (50 to 75% damage), and 4 = severe damage (>75% damage).

The values of liver damage were obtained by evaluating the morphological changes concerning the classic hepatic lobule: (a) uniform distribution of hepatocyte cords that radiate towards the central vein, (b) sinusoidal capillaries that appear as clear regions between the cords of hepatocytes, and (c) hepatocytes with round nuclei and an acidophilic cytoplasm. The evaluated alterations were vascular congestion, lipid vacuoles, and cell degeneration related to necrosis and apoptosis. Regarding the evaluation of renal damage, the morphological changes were evaluated in the renal cortex, mainly comprising glomeruli and proximal tubules (convoluted and straight), where the main functions of the kidney are performed: blood filtering and the generation of primary urine. The evaluated alterations were the degeneration of proximal tubules, tubular atrophy, vascular congestion, and the dilation of the space of Bowman.

2.6. Statistical Analysis

Descriptive statistics were used to determine if they met the normality criteria to analyze the data from the morphometrical analysis of the histopathological analysis. For the data that met the normality criteria, a one-way analysis of variance (ANOVA where $p < 0.05$) and a Tukey–Kramer comparison of means ($p < 0.05$) were used. For data that did not meet the normality criteria, a non-parametric Kruskal–Wallis analysis of variance ($p < 0.05$) and Dunn's multiple comparison ($p < 0.05$) were used to determine the differences among treatments. Statistical analysis was performed using the NCSS 2007 statistical software package, version 1 (NCSS LLC, Kaysville, UT, USA).

3. Results

3.1. Liver

3.1.1. Histological Analysis

In Figure 1, H&E-stained liver photomicrographs of the CBH-treated MS-inducing groups (Figure 1C–E) are presented in contrast to the healthy control group (STD; Figure 1A) and with induction to MS (MS + HC; Figure 1B), as well as the comparative CAR group (Figure 1F). The histological evaluation of the liver of the STD group presented a microanatomy characteristic of normal liver tissue, where polygonal cords of hepatocytes with round euchromatic nuclei and acidophilic cytoplasm are separated by sinusoidal capillaries that uniformly and radially flow to the central vein (Figure 1A). In contrast, liver cells of the MS + HC group showed degeneration, scattered necrotic cells, congestion in the central vein, and lipid vacuoles (Figure 1B).

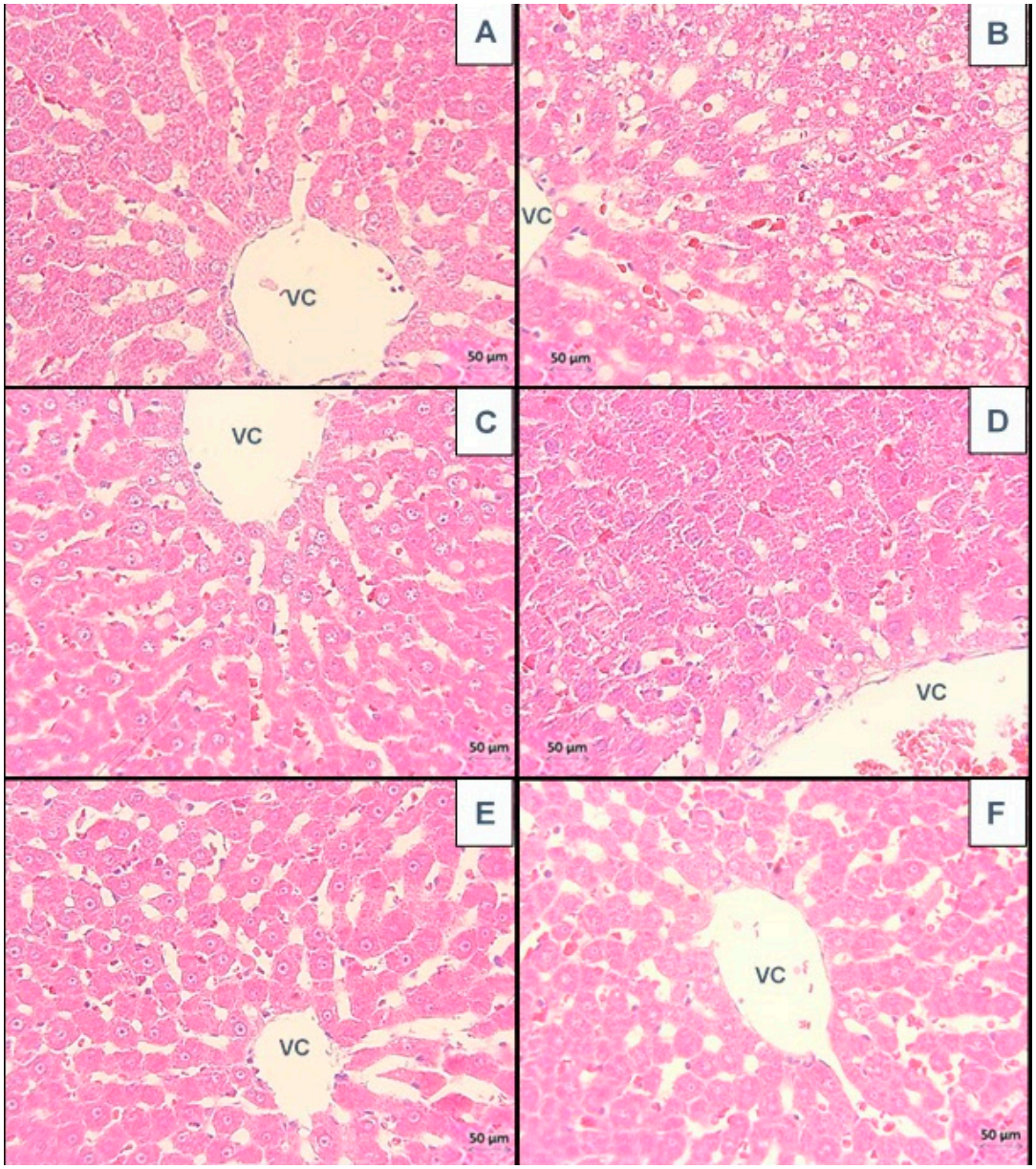

Figure 1. Histological photomicrographs of liver sections from all the groups. (**A**) STD, (**B**) MS + HC, (**C**) CBH-BP: 200 mg/kg, (**D**) CBH-BK: 200 mg/kg, (**E**) CBH-BRO: 200 mg/kg, and (**F**) CAR: 50 mg/kg. VC: central vein. H&E, 40×. Scale bar: 50 µm. Deep blue-violet: nucleus (genetic material). Orange-pink or rose-pink: cytoplasm, collagen, connective tissue, and other structures that surround and support the cell. Observed that CBH-treated groups show better morphology in the liver than the MS + HC group, similar to the STD control group.

Interestingly, the groups treated with CBH showed that a therapeutic effect on the cellular lesions was generated, in contrast to the MS + HC group. Moreover, a decrease in lipid vacuoles was observed in the groups treated with CBH and CAR, in addition to a decrease in the morphological damage generated by the induction of MS (Figure 1C–F).

Figure 2 shows the photomicrographs of the experimental treated groups with CBH and stained with MTS (Figure 2A–F). This staining demonstrated the normal arrangement of collagen fibers in the connective tissue, observing a normal distribution of the liver parenchyma. Therefore, the presence of liver fibrosis was discarded in all the experimental groups evaluated by MTS.

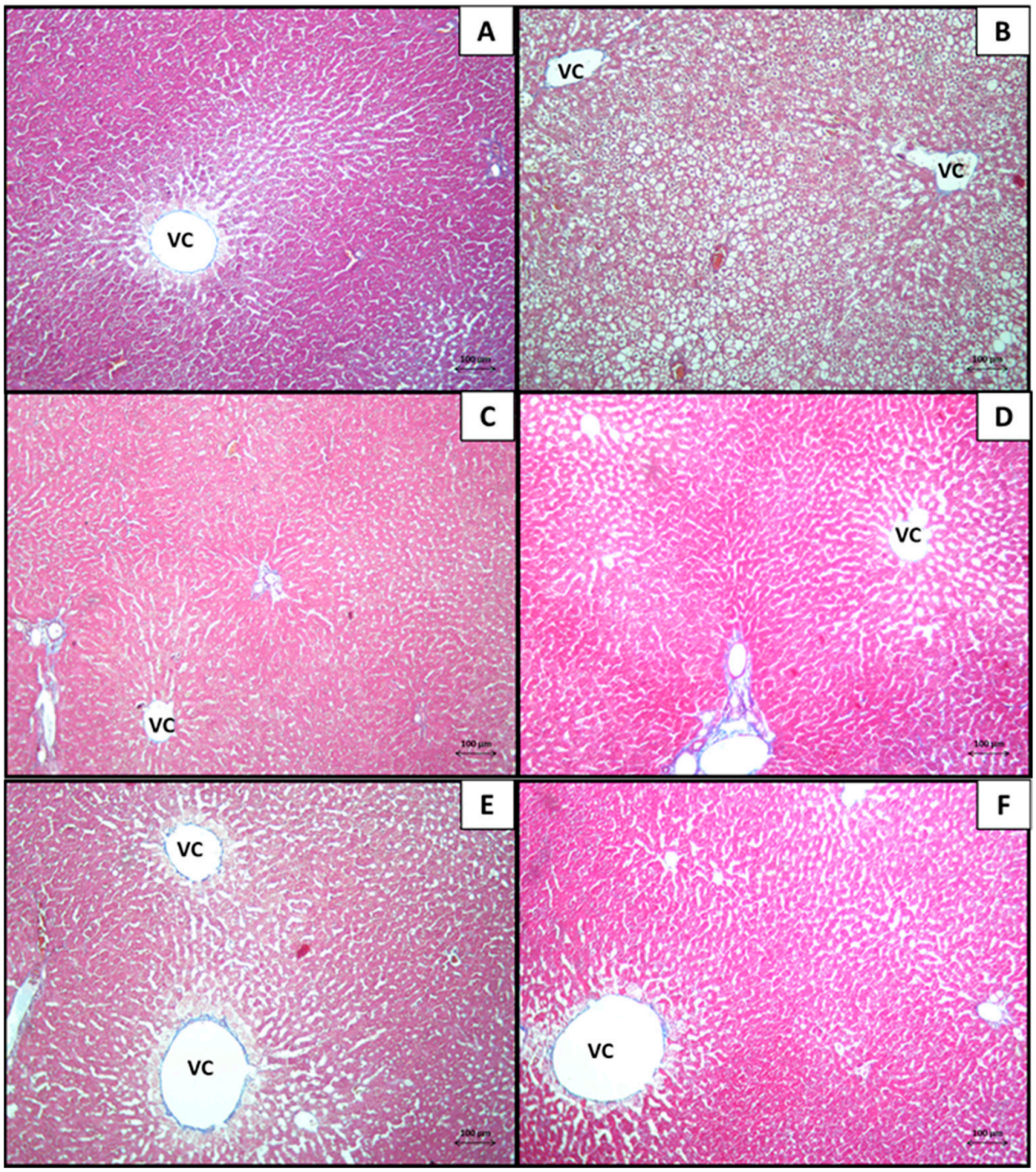

Figure 2. Histological photomicrographs of liver sections from all the groups. (**A**) STD, (**B**) MS + HC, (**C**) CBH-BP: 200 mg/kg, (**D**) CBH-BK: 200 mg/kg, (**E**) CBH-BRO: 200 mg/kg, and (**F**) CAR: 50 mg/kg. VC: central vein. MTS, 10×. Scale bar: 100 µm. Red: collagen fibers in red. Green: elastic fibers. Pink or violet: muscle cells. Fibrosis signals were not observed in all the MS-treated groups. We observed an extensive presence of vacuoles in the MS-HC group.

In Figure 3, the livers of the CBH-treated MS-inducing groups are presented and were analyzed with PAS histochemistry (Figure 3A–F). The cytoplasm of the hepatocytes reacted positively to this method and a qualitative decrease in glycogen was evidenced in the hepatocytes of the rats in the MS + HC group.

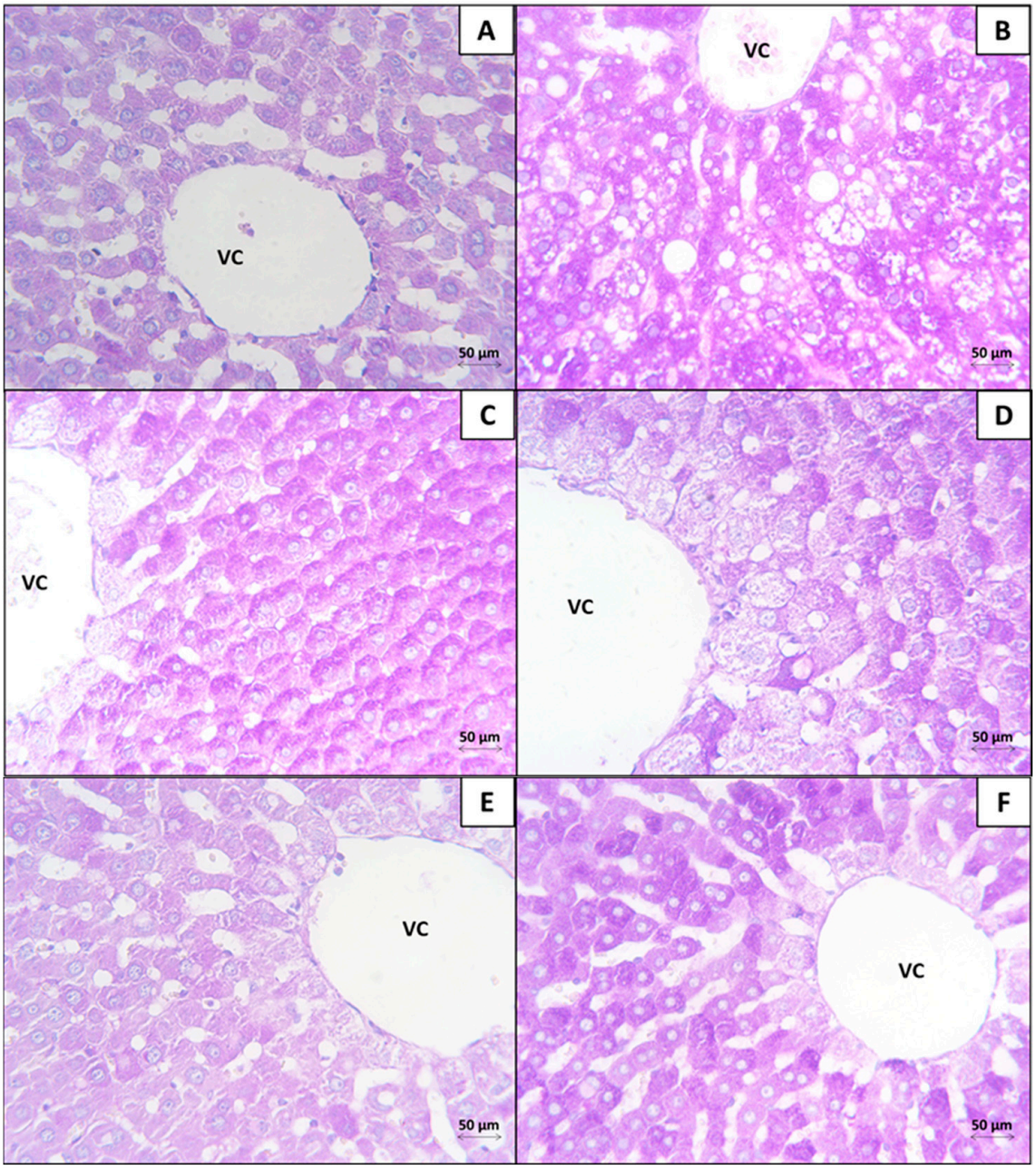

Figure 3. Histological photomicrographs of liver sections from all the groups. (**A**): STD, (**B**): MS + HC, (**C**): CBH-BP: 200 mg/kg, (**D**): CBH-BK: 200 mg/kg, (**E**) CBH-BRO: 200 mg/kg, and (**F**): CAR: 50 mg/kg. VC: central vein. PAS, 40×. Scale bar: 50 µm. Carbohydrates: deep pink to fuchsia. Nuclei: dark blue. Interestingly, the positivity decreased in the MS + HC group, compared to the CBHS-treated groups.

This technique was used to determine the cell lesions related to the decrease in glycogen deposits that were generated by an increase in lipid vacuoles in the groups with MS induction. Our results showed that the groups treated with CBH presented glycogen deposits similar to the healthy group (STD) and an increase in glycogen, in contrast to the MS + HC group.

3.1.2. Morphometrical Analysis of the Histopathological Findings in the Liver

Figure 4 shows the scores of morphological changes in the liver tissues of each group, according to the severity scale of the alterations evaluated: vascular congestion, lipid vacuoles, and cellular alteration.

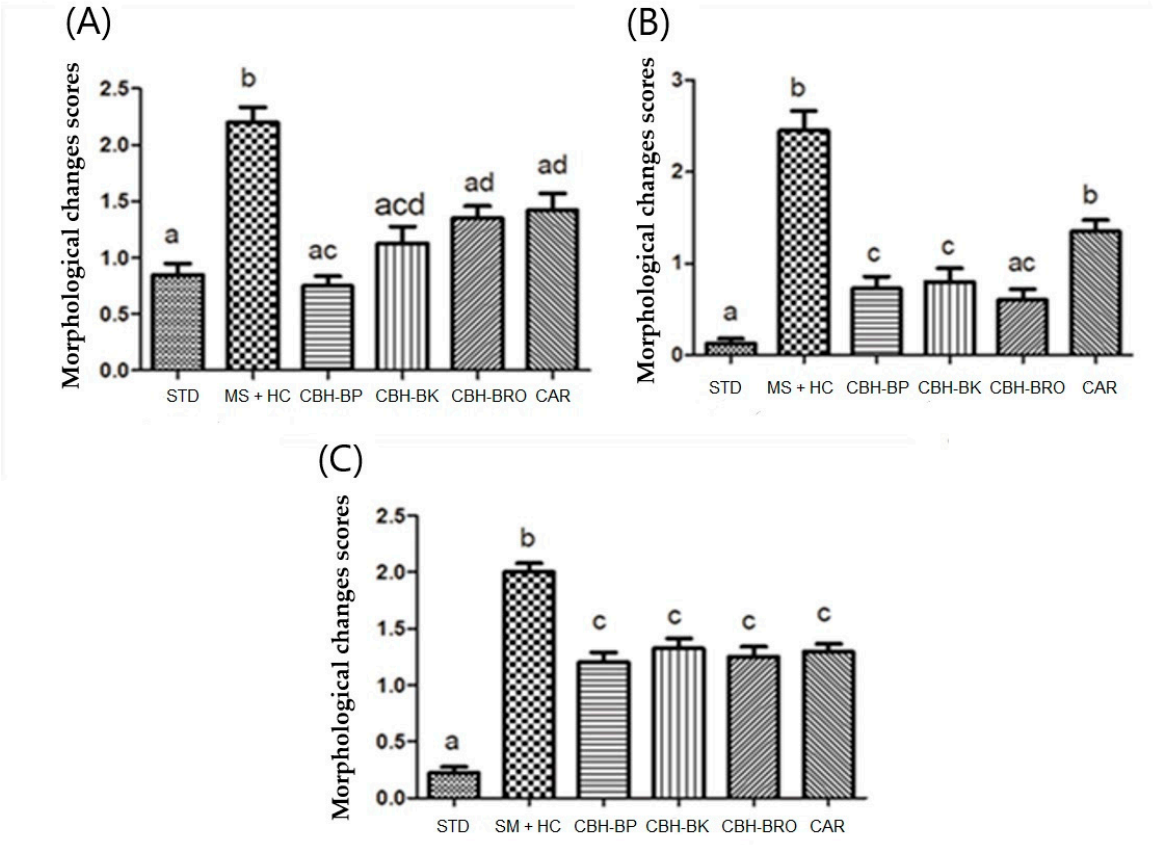

Figure 4. Scores of morphological changes in the livers of each group (n = 5). Vascular congestion (**A**), lipid vacuoles (**B**), cell disruption (**C**), score = 0: no damage, 1: minimal (<25%), 2: mild (25–50%), 3: medium (50–75%), 4: severe (>75%). The mean of scores ± SD. Different letters signify significant differences (Dunn's multiple comparisons, $p < 0.05$).

This morphometric analysis was performed to quantify the cell lesions, related to the decrease in glycogen deposits generated by an increase in lipid vacuoles in the groups with MS induction. Our results showed that the groups treated with CBH presented glycogen deposits similar to the healthy group (STD) and an increase in glycogen, in contrast to the SM + HC group (Figure 4).

The sections evaluated from the group with MS showed the greatest morphological changes ($p < 0.05$) with a multifocal distribution of lipid inclusions (score = 2.5; Figure 4B) and vascular congestion (score = 2.2; Figure 4A), observing a mild cellular alteration (score = 2.0; Figure 4C). The groups treated with CBH presented minimal morphological alterations of lipid vacuoles (<25%) to slight (25–50%) (Figure 4B).

In the evaluation of vascular congestion (Figure 4A) and cellular alteration (Figure 4C), we observed scores < 2, observing a decrease in the alterations evaluated, in comparison with the MS + HC group. In the groups treated with CBH and CAR, a decrease in lipid inclusions (Figure 4B), vascular congestion (Figure 4A), and cellular alteration (Figure 4C) was observed. The liver from the animals treated with CBH-BP and CBH-BK significantly decreased vascular congestion (Figure 4A) and distribution of lipid inclusions (Figure 4B), compared to the CBH-BRO and CAR group. The group treated with CBH-BP did not present significant differences ($p < 0.05$) compared to the healthy group (STD), which showed a decrease in vascular congestion (Figure 4C).

3.2. Kidney

3.2.1. Histopathological Analysis

In Figure 5, the CBH-treated MS-inducing groups (Figure 5C–E) are shown in contrast to the STD group (STD; Figure 5A), the MS + HC (Figure 5B), and the comparative CAR group (Figure 5F). The kidneys from the STD group showed normal histology in the cortex structures: tissular integrity in vessels and tubules, with neither signs of inflammation nor edema (Figure 5A) with slight vascular congestion (Figure 5A). In contrast, the MS + HC group showed increased vascular congestion, tubular necrosis, lumen loss, and generalized tubular necrosis with a loss of the brush border in the proximal convoluted tubules (PCT) (Figure 5B). Also, it had segmented lesions in some glomeruli and dilation of the space of Bowman.

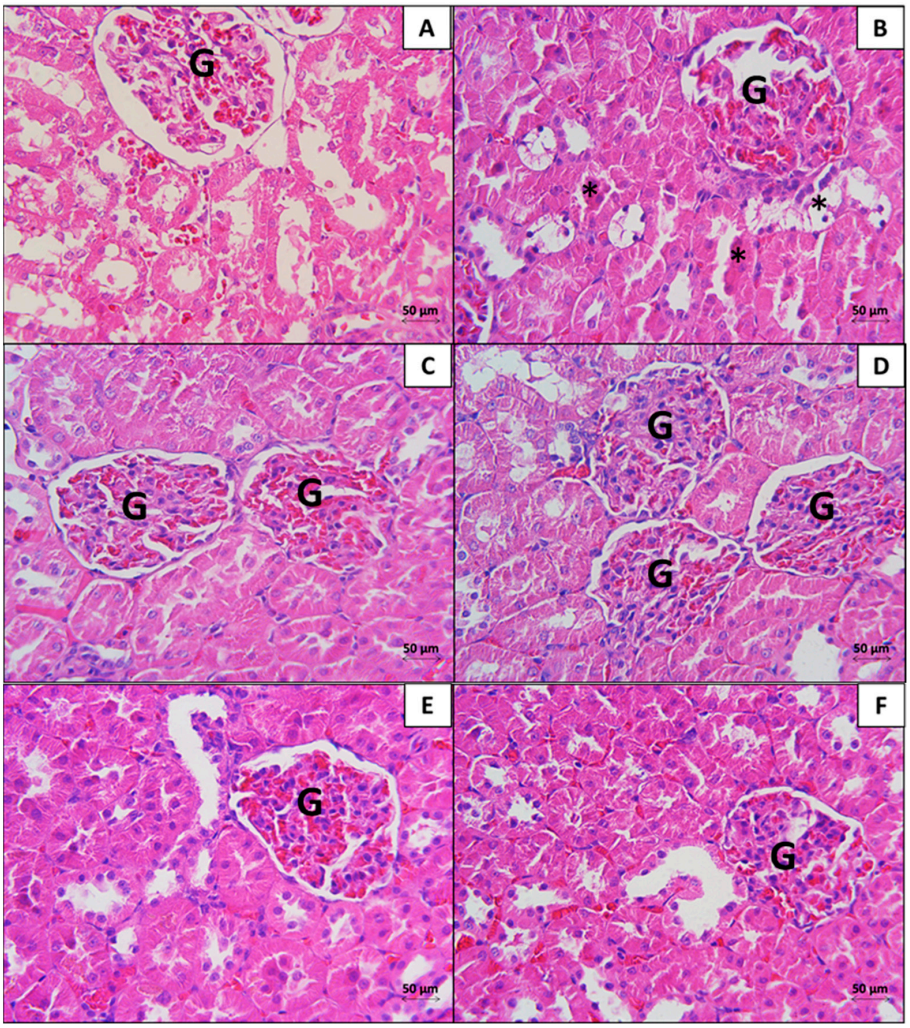

Figure 5. Histological photomicrographs of kidney cortex from all the study groups. (**A**): STD, (**B**): MS + HC, (**C**): CBH-BP: 200 mg/kg, (**D**): CBH-BK: 200 mg/kg, (**E**) CBH-BRO: 200 mg/kg, and (**F**): CAR: 50 mg/kg. Glomerulus (G), Cellular alteration (*). H&E, 40×. Scale bar: 50 µm. Deep blue-violet: nucleus (genetic material). Orange-pink or rose-pink: cytoplasm, collagen, connective tissue, and other structures that surround and support the cell. We observed that CHB-treated groups show better morphology in the kidney than the MS + HC group, similar to the STD control group.

The evaluated kidneys of the groups treated with CBH (Figure 5C–E), and CAR (Figure 5F) showed a decrease in vascular congestion, signs of tubular necrosis (pyknotic nuclei) with a loss of the brush border in some PCT, focalized glomerular deterioration, and dilation of the space of Bowman. All the experimental groups showed vascular congestion

and mild glomerular damage (<25% damage). The damage was focused on the PCT, which presented signs of tubular necrosis: epithelial cells with pyknotic nuclei, ruptured membranes, and a loss of the brush border.

The nephropathy developed by the multiple factors of MS can generate morphological alterations, cellular lesions in the renal corpuscle, and expansion of the glomerular extracellular matrix, characterized by the thickening of the glomerular basement membrane and the increase in deposition of collagen type IV by the mesangial cells [23]. In this sense, the MTS method was performed for the histopathological evaluation of the different experimental groups (Figure 6A–F). The findings with this staining demonstrated the normal disposition of the collagenous fibers of the basal membrane, observing a normal distribution in the renal cortex in all the experimental groups. Therefore, the presence of glomerular fibrosis was discarded in all the experimental groups.

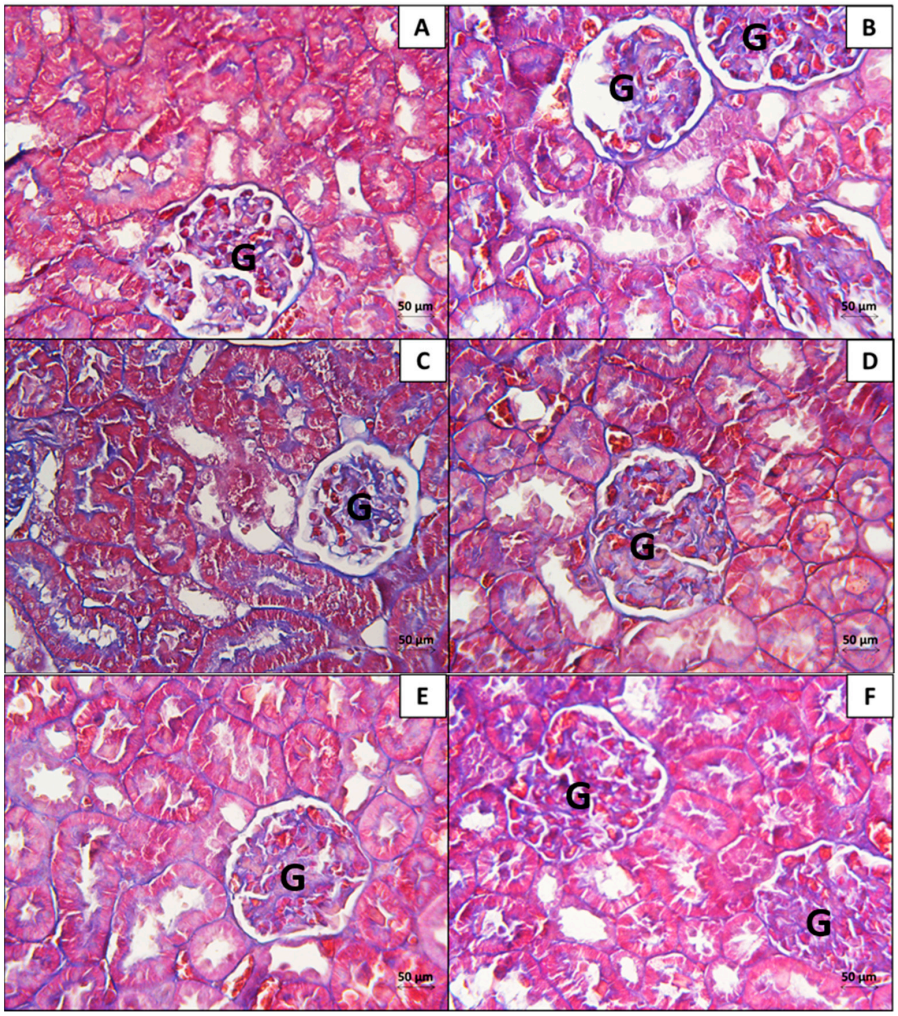

Figure 6. Histological photomicrographs of kidney cortex from all groups. (**A**): STD, (**B**): MS + HC, (**C**): CBH-BP: 200 mg/kg, (**D**): CBH-BK: 200 mg/kg, (**E**) CBH-BRO: 200 mg/kg, and (**F**): CAR: 50 mg/kg. VC: central vein. Glomerulus (G). MTS, 10×. Scale bar: 50 µm. Red: collagen fibers in red; green: elastic fibers. Pink or violet: muscle cells. None of the MS-treated groups exhibited fibrosis signals.

The earliest cell lesions in the development of nephropathy consisted of thickening of the basal glomerular membrane, mesangial expansion, and hyaline accumulation in the arterioles [24]; for this reason, we employed the PAS histochemical technique to evaluate these morphological alterations. Figure 7 shows the findings in the kidneys of groups with the induction of MS and treated with CBH (Figure 7C–E), in contrast to the other experimental groups.

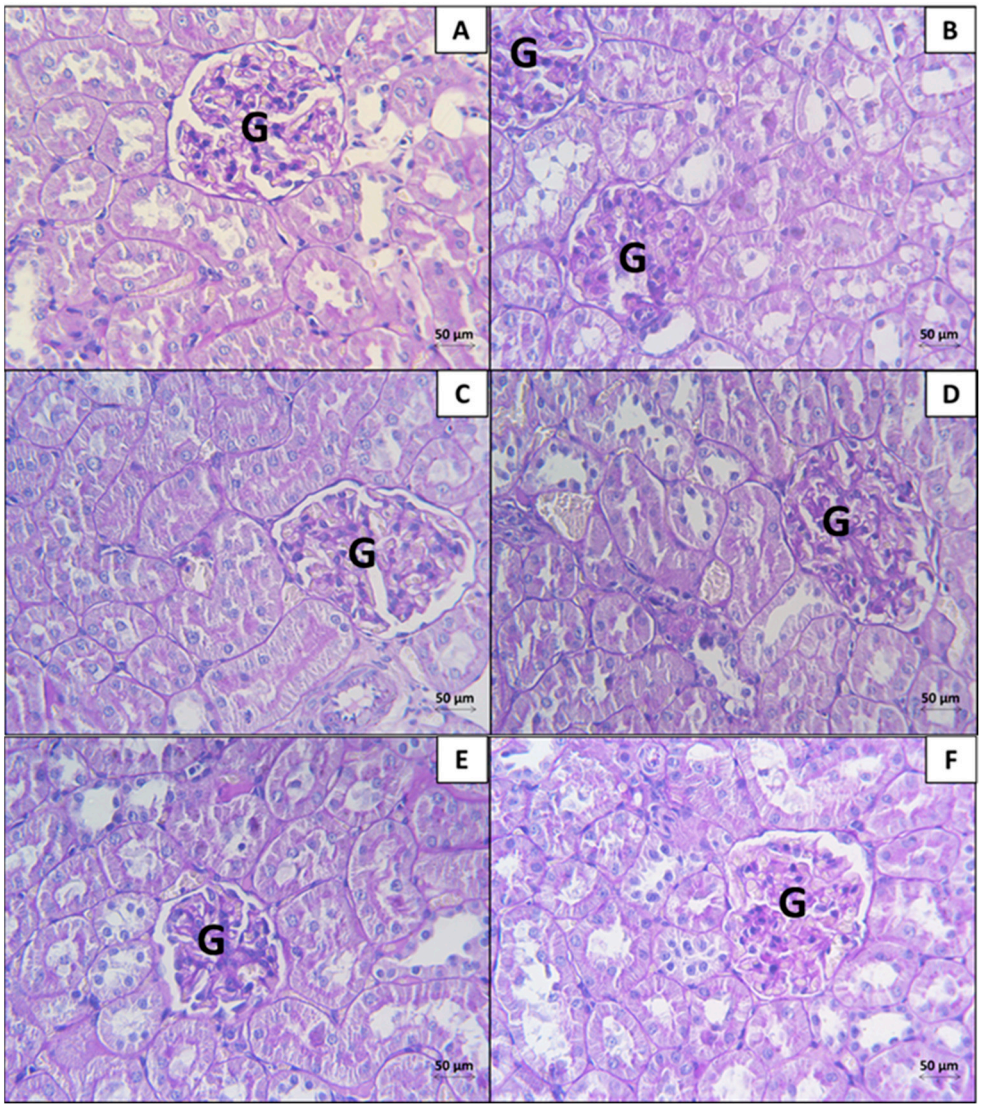

Figure 7. Histological photomicrographs of kidneys of the groups. (**A**) STD, (**B**) MS + HC, (**C**) CBH-BP: 200 mg/kg, (**D**) CBH-BK: 200 mg/kg, (**E**) CBH-BRO: 200 mg/kg, and (**F**) CAR: 50 mg/kg. Glomerulus (G). PAS, 40×. Scale bar: 50 µm. Carbohydrates: deep pink to fuchsia. Nuclei: dark blue. The structural integrity of the basement membrane that covers the glomeruli was maintained in the groups with SM + HC, ruling out pathological thickening.

PAS-positivity is observed in the cellular structures with carbohydrates: the basement membrane (glycoproteins) and the microvilli of the PCT (glycocalyx). According to our findings, the thickening of the basement membrane was discarded. We also observed with this method an increase in generalized tubular necrosis with a loss of the brush border in the kidney of the SM + HC group, in contrast to the STD group. The rats treated with CBH and CAR presented a decrease in these cellular alterations.

3.2.2. Morphometrical Analysis of the Histopathological Findings in the Kidney

Figure 8 shows the score of the morphological changes in the kidney cortex. According to the histopathological examinations performed, the STD group showed minimal pathological findings. The MS + HC group presented tubular degeneration (Figure 8A) related to tubular necrosis with a loss of the brush border, tubular atrophy (Figure 8B), multifocalized vascular congestion (Figure 8C), and dilation of the space of Bowman (Figure 8D). The prevalence of nephrotoxicity findings in the group MS + HC was minimal and slight, ranging between 25% and 50%, which is the expected behavior for this model.

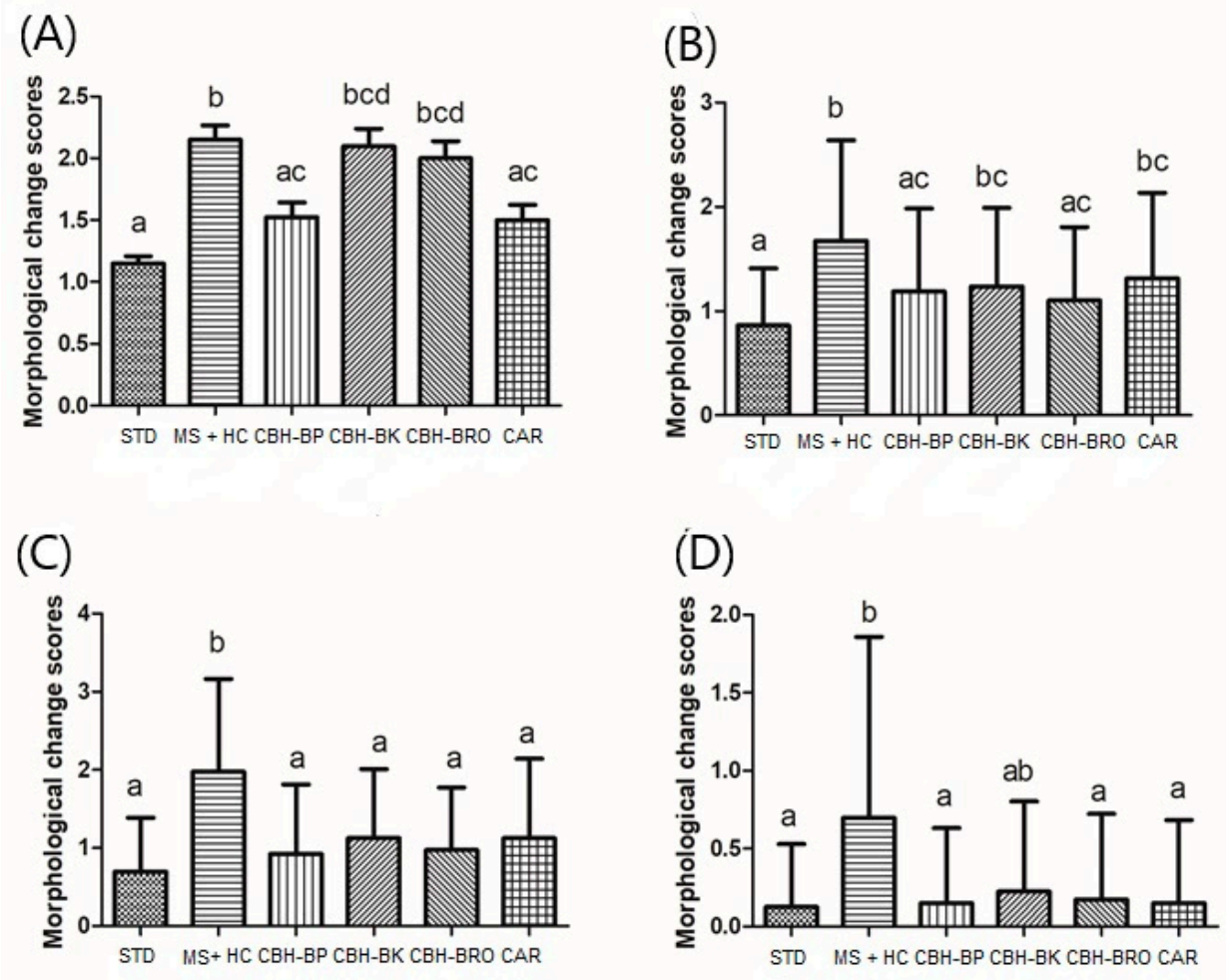

Figure 8. Scores of morphological changes in the kidney. Tubular degeneration (**A**), tubular atrophy (**B**), vascular congestion (**C**), and Bowman's space dilation (**D**). Scoring scale = 0: no damage, 1: minimal (<25%), 2: mild (25–50%), 3: medium (50–75%), and 4: severe (>75%). The mean of scores ± SD. Different letters mean significant differences (Dunn's multiple comparisons, $p < 0.05$).

Mild pathological findings (minimum damage < 25%) were observed in samples of the CBH and CAR-treated groups ($p > 0.05$), presenting a total score < 2. All CBH and CAR treatments, except CBH-BK, did not demonstrate significant differences compared to the STD group; however, CBH-BP and CAR (score = 1.5) were the treatments that presented results closest to the STD group (score = 2). This means that the effect of hydrolysates on kidney morphology is minimal but significant, similar to the effects of CAR (β-alanyl-L-histidine). The histopathological results evidence a therapeutic effect of the bioactive peptides present in the CBH over the morphological alterations in the kidney generated by the presence of MS.

4. Discussion

Bioactive peptides, upon entering the body, interact with specific receptors in liver and kidney cells. Their unique molecular structure allows them to trigger a cascade of intracellular biochemical reactions, resulting in various protective and regulatory effects at the genetic level. Figure 9 presents a schematic diagram that illustrates the possible mechanisms of action proposed for CBH to generate a therapeutic effect on the liver and kidney, which will be explained in Sections 4.1 and 4.2.

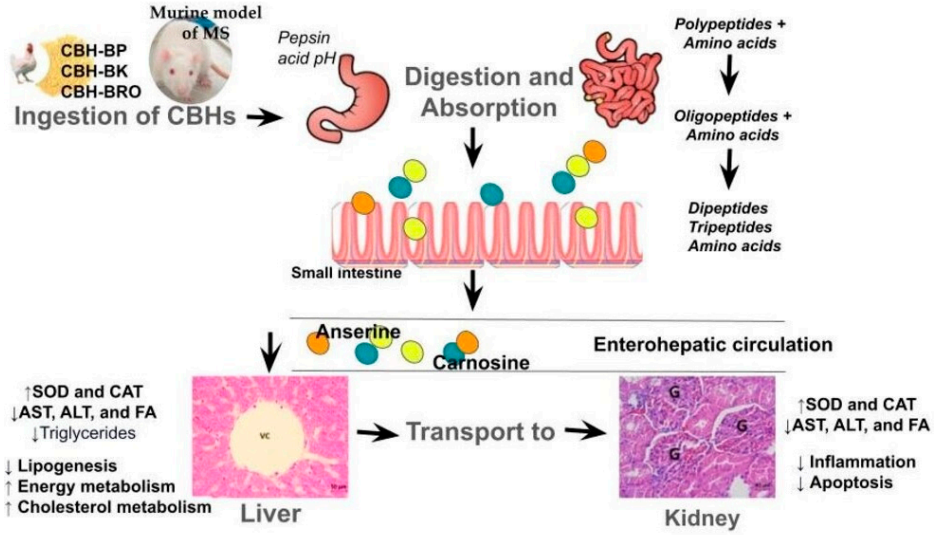

Figure 9. Schematic diagram that illustrates the possible mechanisms of action proposed for CBH to generate a therapeutic effect on the liver and kidney.

4.1. Liver

The histological analysis of the liver in the murine model of MS treated with CBHs provides crucial evidence of their efficacy in preventing or mitigating liver damage associated with the disease. The results of H&E staining revealed a significant decrease in lipid inclusions in the CBHs and CAR groups compared to the MS + HC group, corroborating the observed improvement in serum lipid profiles in murine models of MS after ingesting CBHs [21].

These findings suggest a potential link between CBHs and decreased hepatic lipid accumulation, uptake, or both. Additionally, CBHs may enhance the liver's endogenous antioxidant capacity [20]. This is supported by prior research demonstrating the therapeutic effects of chicken liver hydrolysates on liver fibrosis, attributed to enhanced endogenous antioxidant activities (SOD and CAT) and downregulation of genes and proteins associated with the TGF-β pathway [25]. Similar mechanisms have been described in the prevention of alcoholic fatty liver disease, involving increased antioxidant capacity, regulation of lipid homeostasis, and reduced hepatic inflammation [18].

Moreover, carnosine, a dipeptide abundant in chicken byproduct hydrolysates, has documented antioxidant and lipid-lowering properties, offering additional protection against liver injury [26,27]. Anserine, another dipeptide present in these hydrolysates, has been associated with a decrease in oxidative stress, potentially contributing to the observed hepatoprotective effects [28].

It is important to note that the SM model presented hepatic steatosis, a condition that precedes hepatic fibrosis. This process likely involves the activation of hepatic stellate cells by proinflammatory and fibrogenic cytokines released by Kupffer cells, along with the presence of apoptotic fragments and ROS within hepatocytes [29]. CBHs demonstrated a protective effect, preserving the normal lobular architecture of the liver and reducing distortion and fibrosis. This is particularly significant as advanced liver fibrosis is a severe complication of MS.

The results of PAS histochemistry suggest a positive effect of CBH supplementation, with a decrease in cellular lesions and an increase in glycogen stores in hepatocytes. This could be related to the action of the peptides and amino acids present in CBHs on the β-oxidation of fatty acids. β-oxidation is a key metabolic pathway for the degradation of fatty acids, and its activation can have several benefits, including avoiding excessive fat accumulation in the liver and preventing hepatic steatosis.

The morphometrical analysis of the histopathological findings in the liver of rats with MS provides valuable insights into the potential therapeutic effects of protein hydrolysates

(CBHs). This technique allows for the observation and quantification of morphological and structural alterations in the liver tissue, as well as the determination of the effectiveness of CBHs in preventing or reversing these changes.

The results obtained in this study are consistent with those reported by Lin et al. [17], who observed that groups treated with chicken liver hydrolysates in a murine model of fatty liver demonstrated improved liver lesions by decreasing lipid inclusions and ALT and FA enzyme levels. The possible role of peptides in attenuating cell lesions may be related to the regulation of genes involved in lipid metabolism (PPARα, RXRα, CPT1, and UCP2) and the increment in endogenous antioxidant activity (SOD and CAT). The downregulation of lipogenesis and the upregulation of fatty acid β-oxidation may contribute to decreased serum triglyceride levels and decreased lipid inclusions in the liver [20]. Similar results were observed in this study.

The present study provides compelling evidence that CBHs can effectively prevent or mitigate MS-associated liver damage. The observed reduction in lipid inclusions, together with improvements in serum lipid profiles and enhanced antioxidant capacity, suggests that CBHs may exert their therapeutic effects through multiple mechanisms. Future research should focus on conducting randomized controlled trials in human patients with MS to confirm the efficacy of CBHs and determine the optimal dosage and administration regimens. Furthermore, further investigation into the molecular mechanisms underlying the hepatoprotective effects of CBHs may lead to the development of novel therapeutic strategies for liver diseases.

4.2. Kidney

Each component of MS is an individual risk factor that can lead to the development of kidney diseases, as well as liver lesions. In this sense, the glomeruli, which perform the most important function in filtration, are exposed to numerous factors of injury by MS, such as the presence of arterial hypertension, hyperglycemia, hyperlipidemia, and systematic inflammation that can lead to kidney damage [30]. For this reason, histological evaluation of the kidney in rats with MS can provide valuable information on the mechanisms by which MS damages the kidney and on the effectiveness of possible therapeutic interventions. Employing the H&E, which is considered a basic technique in the evaluation of cellular morphology, the main morphological alterations presented by the model with MS (vascular congestion, generalized tubular necrosis with a loss of the brush border in TCP) were determined as well as the possible therapeutic effects on the altered morphology in the kidney due to the development of MS. The findings found in the present investigation did not reveal evidence of glomerular fibrosis in any of the experimental groups that used the MTS technique. This result may be due to the early stage of metabolic syndrome development in our animal model. Nephropathy, a common complication of metabolic syndrome, is characterized by morphological alterations, cellular lesions in the renal corpuscle, and expansion of the glomerular extracellular matrix. These changes often include thickening of the glomerular basement membrane and increased type IV collagen deposition by mesangial cells [23]. Although the MTS technique can be a valuable tool to evaluate these changes in histological sections, it may not be sensitive enough to detect early-stage fibrosis.

Likewise, previous research showed that glomerular basement membrane (GBM) thickening, mesangial expansion, and hyaline accumulation in arterioles are early signs of nephropathy development [31]. Therefore, in the present investigation, the PAS histochemical technique was used to evaluate these specific changes. Our findings did not reveal GBM thickening. This alteration is typically characterized by a thickened capillary wall due to various deposits, including immune complexes, fibrin, and amyloid cryoglobulins, along with the increased synthesis of basement membrane components [24]. These changes usually reflect a pathological response of the glomerulus to an injury. The absence of GBM thickening in our study suggests that the observed damage could be at an earlier stage or may involve different mechanisms compared to established nephropathy models.

Similarly, in our analysis, no mesangial expansion was observed within the renal cortex, another indicator of nephropathy. In contrast, our study identified a loss of the brush border in the PCT. This loss can significantly compromise the reabsorption function of the PCT, which is critical for reclaiming essential solutes like sodium (Na+) (around 65%), glucose, amino acids, and water (approximately 95%) from the filtrate [32]. Additionally, the PCT plays a vital role in excreting toxins from the filtered blood plasma back into the bloodstream. A loss of the brush border disrupts these vital reabsorption and secretion processes, potentially leading to electrolyte imbalances, disrupted blood sugar control, and impaired waste product elimination. Further investigations are warranted to elucidate the underlying mechanisms leading to the observed loss of the PCT brush border and its potential functional consequences. Additionally, exploring other markers associated with nephropathy progression could provide a more comprehensive understanding of the disease process in this context.

Animal studies have shown that chicken byproduct hydrolysates may have beneficial effects on cardiovascular and metabolic health. However, evidence of the effect of CBH on renal function in the context of MS is limited. In this sense, a histopathological evaluation of the kidney is an important tool to evaluate kidney damage in the model with SM, identify the mechanisms underlying kidney damage, and determine the effectiveness of therapeutic interventions, to evaluate the possible therapeutic effects of the CBHs in the model with MS. Moreover, some studies have indicated that proximal tubular cells have specific transport systems for dipeptides and tripeptides. Di- and tripeptides, which are filtered in the glomerulus and include those that are produced from larger polypeptides by the action of brush border peptidases, are the substrates for the renal peptide transport system under physiological conditions [10,33]. This could be related to the greater availability of the di- and tripeptides and the therapeutic effect that CBHs and CARs are generating in the groups of rats with MS in the present investigation. To our knowledge, there are no similar histopathological studies on the renoprotective effect of hydrolysates from chicken byproducts in murine models with MS like that observed in the present study; however, there are recent studies on the evaluation of the renoprotective effect of peptides derived from various protein sources, and some authors suggest that small peptides, as multifunctional biomolecules, can positively affect some organs and metabolic disorders [10].

Recently, the study of the therapeutic effect of some di- and tripeptides has become important, because some di- and tripeptides have been related to a better rate of absorption, and their presence in the blood has been identified after the consumption of sources rich in proteins and peptides. Also, some di- and tripeptides can present specific biological activities [34–36]. Additionally, it has been reported that the dipeptides of CAR and Hannaneh (Leu-Gly) generate a protective effect, presenting a decrease in enzymatic activities (AST, ALT, and FA) in the kidney related to cell lesions. They also favor antioxidant activity (SOD and CAT) and decrease histological renal abnormalities in diabetic mice [4]. In this sense, the renoprotective effect of dipeptides and tripeptides composed of proline, glycine, leucine, alanine, and histidine was demonstrated in diabetic mice, which is mainly attributed to the anti-inflammatory and antioxidant activities they present [37]. The renoprotective effect of the bioactive peptide Val-His-Val-Val from soy has also been reported, attributed to the suppression of inflammation and apoptosis, and the restorative effect on kidney architecture after treatment with peptides showed therapeutic effects by decreasing kidney damage caused by free radicals [38]. The present research opens avenues for future investigations into the specific mechanisms by which the dipeptides and tripeptides present in CBHs and CARs exert their renoprotective effects. Future research could focus on identifying and quantifying the specific peptide components responsible for these beneficial effects and elucidating their precise signaling pathways within the kidney.

This study provides valuable insights into the potential renoprotective effects of CBHs in the context of MS. These findings demonstrate that CBHs may mitigate kidney damage by preserving the integrity of the PCT and preventing the development of glomerular fibrosis. These effects could be attributed to the presence of dipeptides and tripeptides within CBHs,

which may exert antioxidant, anti-inflammatory, and renoprotective activities. Future research is needed to explore other markers associated with the progression of nephropathy, which would favor a more comprehensive understanding of the renoprotective potential of CBHs in MS.

4.3. Limitations of This Study

4.3.1. Generalization of the Animal Model

The use of Wistar rats as an animal model, although common, has limitations in terms of its extrapolation to the human phenotype of metabolic syndrome. Genetic heterogeneities, variations in diet, and environmental factors inherent to each species can introduce biases in the results obtained. Additionally, interindividual variability within each experimental group can significantly influence the response to treatment.

4.3.2. Technical Limitations of Histological Analysis

Histopathological evaluation, despite being a valuable tool, is subject to certain inherent limitations. The intrinsic subjectivity in the assignment of scores, influenced by the experience of the observer, can introduce variability in the results. Likewise, the focus of this study on liver and kidney tissue limits the comprehensive understanding of the effects of treatment, given that other key organs in the pathophysiology of metabolic syndrome, such as the pancreas and adipose tissue, were not evaluated. In future studies, it would be useful to complement the histopathological analysis with molecular techniques for a more in-depth characterization of the mechanisms underlying the observed effects.

4.3.3. Potential Clinical Applications

CBHs could be used as an adjunctive therapy to complement existing MS treatments, potentially improving liver and kidney function and overall quality of life. They could also be explored as a preventative measure for people at risk of developing MS, such as those with metabolic risk factors or a family history of the disease. They could also be incorporated into personalized nutrition plans for people with MS, providing specific nutritional support for liver and kidney health.

5. Conclusions

The present study provides compelling preclinical evidence suggesting that chicken byproduct hydrolysates (CBHs) derived from plant proteases may benefit the hepatic and renal tissues of mice with metabolic syndrome (MS). Histological and histopathological analyses demonstrated that CBH treatments are associated with improvements in liver and kidney morphology, including a reduction in inflammation and steatosis. These findings collectively suggest that CBHs characterized by a mixture of low and high-molecular-weight peptides could potentially serve as a promising therapeutic modality for MS. However, further investigations in human populations are imperative to validate these preclinical observations and to establish the optimal dosage and treatment regimen of CBHs for the clinical management of MS.

Author Contributions: Conceptualization, M.G.R.-G., C.R.-A. and M.d.L.G.-M.; methodology, A.S.-D. and O.S.-C.; validation, A.S.-D., C.R.-A. and M.d.L.G.-M.; formal analysis, M.G.R.-G.; investigation, M.G.R.-G.; data curation, M.G.R.-G. and A.S.-D.; writing—original draft preparation, M.G.R.-G. and A.S.-D.; writing—review and editing, E.M.-G., E.M.B.-V., O.S.-C., C.R.-A. and M.d.L.G.-M.; supervision, A.S.-D. and O.S.-C.; project administration, A.S.-D., C.R.-A. and M.d.L.G.-M. All authors have read and agreed to the published version of the manuscript.

Funding: This research received no external funding.

Institutional Review Board Statement: The animal study protocol was approved by the Institutional Review Board of Tecnológico Nacional de México/Instituto Tecnológico de Tepic (experimental protocol: M00.2./471/2019) on 11 March 2019. Likewise, the State Bioethics Committee of Nayarit, Mexico approved the experimental protocol (No. CENB/03/2017) used in the present investigation, and the protocols of the Institutional Committee for the Care and Use of Animals were performed according to the Mexican standards (NOM-062-ZOO-1999, 2017).

Informed Consent Statement: Not applicable.

Data Availability Statement: The data presented in this study are available in this article.

Acknowledgments: The authors thank the Tecnológico Nacional de México (project code 5565.19-P) for their support in this project. The authors also wish to thank CONACYT (Mexico) for the scholarship awarded to Martha Guillermina Romero Garay (scholarship number: 287441).

Conflicts of Interest: The authors declare no conflicts of interest.

References

1. Suman, R.K.; Mohanty, I.R.; Borde, M.K.; Maheshwari, U.; Deshmukh, Y.A. Development of an experimental model of diabetes co-existing with metabolic syndrome in rats. *Adv. Pharmacol. Sci.* **2016**, *2016*, 9463476. [CrossRef] [PubMed]
2. Selvan, K.T.; Goon, J.A.; Makpol, S.; Tan, J.K. Effects of Microalgae on Metabolic Syndrome. *Antioxidants* **2023**, *12*, 449. [CrossRef] [PubMed]
3. Ahima, R.S. Overview of metabolic syndrome. In *Metabolic Syndrome: A Comprehensive Textbook*; Springer International Publishing: Cham, Switzerland, 2024; pp. 3–14.
4. Martins, A.D.; Majzoub, A.; Agawal, A. Metabolic syndrome, and male fertility. *World J. Mens. Health* **2019**, *37*, 113–127. [CrossRef]
5. Vidigal, F.d.C.; Bressan, J.; Babio, N.; Salas-Salvadó, J. Prevalence of metabolic syndrome in Brazilian adults: A systematic review. *BMC Public Health* **2013**, *13*, 1198. [CrossRef]
6. Ntamo, Y.; Jack, B.; Ziqubu, K.; Mazibuko-Mbeje, S.E.; Nkambule, B.B.; Nyambuya, T.M.; Mabhida, S.E.; Hanser, S.; Orlando, P.; Tiano, L.; et al. Epigallocatechin gallate as a nutraceutical to potentially target the metabolic syndrome: Novel insights into therapeutic effects beyond its antioxidant and anti-inflammatory properties. *Crit. Rev. Food Sci. Nutr.* **2022**, *64*, 87–109. [CrossRef]
7. Huh, J.H.; Kang, D.R.; Kim, J.Y.; Koh, K.K. Metabolic syndrome fact sheet 2021: Executive report. *Cardiometab. Syndr. J.* **2021**, *1*, 125–134. [CrossRef]
8. Park, N.-Y.; Jang, S. Effects of mHealth Practice Patterns on Improving Metabolic Syndrome Using the Information–Motivation–Behavioral Skills Model. *Nutrients* **2024**, *16*, 2099. [CrossRef]
9. Sánchez, A.; Vázquez, A. Bioactive peptides: A review. *Food Qual. Saf.* **2017**, *1*, 29–46. [CrossRef]
10. Vahdatpour, T.; Valizadeh, H.; Mirzakhani, N.; Mesgari-Abbasi, M. Renoprotective Effects of Di- and Tri-peptides Containing Proline, Glycine and Leucine in Diabetes Model of Adult Mice: Enzymology and Histopathology. *Int. J. Pept. Res. Ther.* **2020**, *26*, 2345–2354. [CrossRef]
11. Romero-Garay, M.G.; Montalvo-González, E.; Hernández-González, C.; Soto-Domínguez, A.; Becerra-Verdín, E.M.; García-Magaña, M.D.L. Bioactivity of peptides obtained from poultry by-products: A review. *Food Chem. X* **2021**, *13*, 100181. [CrossRef]
12. Ibarz-Blanch, N.; Alcaide-Hidalgo, J.M.; Cortés-Espinar, A.J.; Albi-Puig, J.; Suárez, M.; Mulero, M.; Morales, D.; Bravo, F.I. Chicken slaughterhouse by-products: A source of protein hydrolysates to manage non-communicable diseases. *Trends Food Sci. Technol.* **2023**, *139*, 104125. [CrossRef]
13. Romero-Garay, M.G.; Martínez-Montaño, E.; Hernández-Mendoza, A.; Vallejo-Cordoba, B.; González-Córdova, A.F.; Montalvo-González, E.; García-Magaña, M.d.L. *Bromelia karatas* and *Bromelia pinguin*: Sources of plant proteases used for obtaining antioxidant hydrolysates from chicken and fish by-products. *Appl. Biol. Chem.* **2020**, *63*, 41. [CrossRef]
14. Lin, Y.-L.; Chen, C.Y.; Yang, D.J.; Wu, Y.H.S.; Lee, Y.J.; Chen, Y.C.; Chen, Y.C. Hepatic-Modulatory Effects of Chicken Liver Hydrolysate-Based Supplement on Autophagy Regulation against Liver Fibrogenesis. *Antioxidants* **2023**, *12*, 493. [CrossRef] [PubMed]
15. Wu, Y.H.S.; Lin, Y.L.; Yang, W.Y.; Wang, S.Y.; Chen, Y.C. Pepsin-digested chicken-liver hydrolysate attenuates hepatosteatosis by relieving hepatic and peripheral insulin resistance in long-term high-fat dietary habit. *J. Food Drug Anal.* **2021**, *29*, 376–389. [CrossRef]
16. Wu, Y.S.; Lin, Y.; Huang, C.; Chiu, C.; Nakthong, S.; Chen, Y. Cardiac protection of functional chicken-liver hydrolysates on the high-fat diet induced cardio-renal damages via sustaining autophagy homeostasis. *J. Sci. Food Agric.* **2020**, *100*, 2443–2452. [CrossRef]
17. Lin, Y.L.; Tai, S.Y.; Chen, J.W.; Chou, C.H.; Fu, S.G.; Chen, Y.C. Ameliorative effects of pepsin-digested chicken liver hydrolysates on development of alcoholic fatty livers in mice. *Food Funct.* **2017**, *8*, 1763–1774. [CrossRef]
18. Chen, P.J.; Tseng, J.K.; Lin, Y.L.; Wu, Y.H.S.; Hsiao, Y.T.; Chen, J.W.; Chen, Y.C. Protective Effects of Functional Chicken Liver Hydrolysates against Liver Fibrogenesis: Antioxidation, Anti-inflammation, and Antifibrosis. *J. Agric. Food Chem.* **2017**, *65*, 4961–4969. [CrossRef]

19. Chou, C.; Wang, S.; Lin, Y.; Chen, Y. Antioxidant activities of chicken liver hydrolysates by pepsin treatment. *Int. J. Food Sci. Technol.* **2013**, *49*, 1654–1662. [CrossRef]
20. Yang, K.T.; Lin, C.; Liu, C.W.; Chen, Y.C. Effects of chicken-liver hydrolysates on lipid metabolism in a high-fat diet. *Food Chem.* **2014**, *160*, 148–156. [CrossRef]
21. Romero-Garay, M.G.; Becerra-Verdín, E.M.; Soto-Domínguez, A.; Montalvo-González, E.; García-Magaña, M.L. Health effects of peptides obtained from hydrolysed chicken by-products by the action of Bromelia pinguin and B. karatas proteases in Wistar rats induced with metabolic syndrome. *Int. Food Res. J.* **2022**, *29*, 1078. [CrossRef]
22. García-Magaña, M.d.L.; González-Borrayo, J.; Montalvo-González, E.; Rudiño-Piñera, E.; Sáyago-Ayerdi, S.G.; Salazar-Leyva, J.A. Isoelectric focusing, effect of reducing agents and inhibitors: Partial characterization of proteases extracted from Bromelia karatas. *Appl. Biol. Chem.* **2018**, *61*, 459–467. [CrossRef]
23. Zafar, M.; Naqvi, S.N.U.; Ahmed, M.; Kaimkhani, Z.A. Altered Kidney Morphology and Enzymes in Streptozotocin Induced Diabetic Rats. *Int. J. Morphol.* **2009**, *27*, 783–790. [CrossRef]
24. Mitchell, J.C.; Kumar, R.N.; Abbas, V.; Aster, A.K.; de Robbins y Cotran, C. *Patologia Estructural y Funcional*; Elsevier: Amsterdam, The Netherlands, 2017.
25. Liu, D.; Chen, X.; Huang, J.; Zhou, X.; Huang, M.; Zhou, G. Stability of antioxidant peptides from duck meat after post-mortem ageing. *Int. J. Food Sci. Technol.* **2017**, *52*, 2513–2521. [CrossRef]
26. Mong, M.-C.; Chao, C.-Y.; Yin, M.-C. Histidine and carnosine alleviated hepatic steatosis in mice consumed high saturated fat diet. *Eur. J. Pharmacol.* **2011**, *653*, 82–88. [CrossRef]
27. Xu, Q.; Hong, H.; Wu, J.; Yan, X. Bioavailability of bioactive peptides derived from food proteins across the intestinal epithelial membrane: A review. *Trends Food Sci. Technol.* **2019**, *86*, 399–411. [CrossRef]
28. Ali, S.A.; Fadda, L.M.; Elebiary, H.; Soliman, M. Evaluation of the radioprotective action of anserine along with zinc in albino rats exposed to gamma-radiation. *J. Appl. Pharm. Sci.* **2012**, *2*, 115–122. [CrossRef]
29. Peverill, W.; Powell, L.W.; Skoien, R. Evolving concepts in the pathogenesis of NASH: Beyond steatosis and inflammation. *Int. J. Mol. Sci.* **2014**, *15*, 8591–8638. [CrossRef]
30. Lizardo, M.E.; del Pilar Navarro, M.; Camacho, M.; Magallanes-Hernández, M.A.; Pacheco-Gutiérrez, R.G.; López-Bordones, M.; Dorta, L. Estimación de la tasa de filtración glomerular en personas con y sin síndrome metabólico. *Rev. Fac. Ciencias Salud UDES* **2016**, *3*, 22–28. [CrossRef]
31. Letelier, C.E.M.; Ojeda, C.A.S.M.; Provoste, J.J.R.; Zaror, C.J.F. Fisiopatología de la nefropatía diabética: Una revisión de la literatura. *Medwave* **2017**, *17*, 6839. [CrossRef]
32. Carracedo, J.; Ramírez, R. Fisiología Renal. 2020, pp. 1–20. Available online: http://www.nefrologiaaldia.org/ (accessed on 5 June 2024).
33. Ganapathy, V.; Leibach, F.H. Carrier-mediated reabsorption of small peptides in renal proximal tubule. *Am. J. Physiol. Physiol.* **1986**, *251*, F945–F953. [CrossRef]
34. Kitada, M.; Ogura, Y.; Koya, D. Rodent models of diabetic nephropathy: Their utility and limitations. *Int. J. Nephrol. Renov. Dis.* **2016**, *9*, 279–290. [CrossRef] [PubMed]
35. Song, H.; Li, B. Beneficial effects of collagen hydrolysate: A review on recent developments. *Biomed. J. Sci. Tech. Res.* **2017**, *1*, 458–461.
36. Vahdatpour, T.; Nokhodchi, A.; Zakeri-Milani, P.; Mesgari-Abbasi, M.; Ahmadi-Asl, N.; Valizadeh, H. Leucine–glycine and carnosine dipeptides prevent diabetes induced by multiple low-doses of streptozotocin in an experimental model of adult mice. *J. Diabetes Investig.* **2019**, *10*, 1177–1188. [CrossRef] [PubMed]
37. Lee, Y.T.; Hsu, C.C.; Lin, M.H.; Liu, K.S.; Yin, M.C. Histidine and carnosine delay diabetic deterioration in mice and protect human low density lipoprotein against oxidation and glycation. *Eur. J. Pharmacol.* **2005**, *513*, 145–150. [CrossRef]
38. Tsai, B.C.K.; Kuo, W.W.; Day, C.H.; Hsieh, D.J.Y.; Kuo, C.H.; Daddam, J.; Chen, R.J.; Padma, V.V.; Wang, G.; Huang, C.Y. The soybean bioactive peptide VHVV alleviates hypertension-induced renal damage in hypertensive rats via the SIRT1-PGC1α/Nrf2 pathway. *J. Funct. Foods* **2020**, *75*, 104255. [CrossRef]